

University of Warsaw  
Faculty of Chemistry

**Piotr Garbacz**

**Załącznik III  
Appendix III**

**Summary of Professional Accomplishments**

Warsaw, July 2018

## Contents

|           |   |           |
|-----------|---|-----------|
| <b>A.</b> | <b>Personal details</b>   | <b>3</b>  |
| <b>B.</b> | <b>Scientific achievement</b>   | <b>3</b>  |
| <b>C.</b> | <b>Publications related to the achievement</b>  | <b>3</b>  |
| <b>D.</b> | <b>Description of the scientific achievement</b>  | <b>5</b>  |
| D.1.      | Introduction  | 5         |
| D.2.      | Significance of the predicted effects for enantiomers discrimination                    | 5         |
| D.3.      | Irreducible spherical decomposition of a tensor   | 7         |
| D.4.      | Hamiltonian of a spin system perturbed by an electric field                             | 7         |
| D.5.      | Relationship between molecular chirality and NMR phenomena involving the electric field | 9         |
| D.6.      | Mathematical framework used to find the effects induced by the $E$ field                | 10        |
| D.7.      | Predicted effect induced by an electric field   | 10        |
| D.8.      | Summary   | 27        |
| D.9.      | References  | 29        |
| <b>E.</b> | <b>Other scientific achievements</b>  | <b>30</b> |

**A. Personal details****A.1. Name and surname**

Piotr Garbacz

**A.2. Held diploma and scientific degrees – with the name, place and year of acquisition and title of Ph.D. dissertation**

2008 – M. Sc. in Chemistry, Faculty of Chemistry, University of Warsaw

2008 – M. Sc. in Biology, Faculty of Biology, University of Warsaw

2010 – M. Sc. in Psychology, Faculty of Psychology, University of Warsaw

2011 – M. Sc. in Physics, Faculty of Physics, University of Warsaw

2011 – B. Sc. in Mathematics, Faculty of Mathematics, Informatics, and Mechanics,  
University of Warsaw

2014 – Ph. D. in Chemistry, Faculty of Chemistry, University of Warsaw

title of the dissertation:

“NMR Studies of Magnetic Shielding in Gaseous Hydrogen and Solid Iridium Hydrides”

**A.3. Previous employment in scientific institutions**

2016 – present     assistant professor, Faculty of Chemistry, University of Warsaw

2014 – 2015       postdoctoral researcher, Max Planck Institute, Stuttgart, Germany

2014 – 2016       assistant, Faculty of Chemistry, University of Warsaw

**B. Indication of achievements according to Art. 16, item 2, Act of 14 March 2003 – Law on Higher Education, the Law on Academic Degrees and Title and Degrees in Art (Journal of Laws No 65, item 595 with further amendments):****Title of the scientific achievement**

“Nuclear magnetic resonance spectroscopy in an electric field”

**C. Publications related to the achievement (habilitation thesis) included in Journal Citation Reports database. In all articles, I am the corresponding author. Impact factors are given according to the year of publication.****H1. P. Garbacz**

"Nuclear relaxation in an electric field enables the determination of isotropic magnetic shielding"

*Journal of Chemical Physics*, 2016, 145, 064202

**MNiSW: 35, IF<sub>2016</sub>: 2.965**

**H2. P. Garbacz**

"The Bloch equation with terms induced by an electric field"

*Journal of Chemical Physics*, 2018, 148, 034501

**MNiSW: 35, IF<sub>2016</sub>: 2.965**

- H3. **P. Garbacz**, A. D. Buckingham  
 "Chirality-sensitive nuclear magnetic resonance effects induced by indirect spin-spin coupling"  
*Journal of Chemical Physics*, 2016, 145, 204201  
**MNiSW: 35, IF<sub>2016</sub>: 2.965**
- My contribution to this work is the main idea of the article, the derivation of the formula, which allows to compute an inducted chirality-sensitive electric polarization from the density matrix of the spin system using the operator  $\chi$ , the design of experiments aiming to observe postulated effects, and CCSD quantum chemistry computations. I wrote the first version of the paper. I estimate my contribution to this work as approximately 65 %.*
- H4. **P. Garbacz**  
 "Chirality-sensitive effects induced by nuclear relaxation in an electric field"  
*Journal of Chemical Physics*, 2016, 145, 224202  
**MNiSW: 35, IF<sub>2016</sub>: 2.965**
- H5. **P. Garbacz**, P. Fischer, S. Krämer  
 "A loop-gap resonator for chirality-sensitive nuclear magneto-electric resonance (NMER)"  
*Journal of Chemical Physics*, 2016, 145, 104201  
**MNiSW: 35, IF<sub>2016</sub>: 2.965**
- My contribution to this work is the main idea of the article, the design of the resonator described in the paper, computations of the  $\mathbf{E}$  and  $\mathbf{B}$  fields distributions using the COMSOL computer program, computations of the spin dynamics in the sample placed inside the resonator. I wrote the first version of the paper. I estimate my contribution to this work as approximately 75 %.*
- H6. **P. Garbacz**  
 "Computations of the chirality-sensitive effect induced by an antisymmetric indirect spin-spin coupling"  
*Molecular Physics* 2018, 116, 1397  
**MNiSW: 20, IF<sub>2016</sub>: 1,870**
- H7. **P. Garbacz**, J. Cukras, M. Jaszuński  
 "A theoretical study of potentially observable chirality-sensitive NMR effects in molecules"  
*Physical Chemistry Chemical Physics*, 2015, 17, 22642  
**MNiSW: 35, IF<sub>2015</sub>: 4.449**
- My contribution to this work is the main idea of the article (in particular, the proposition of the introduction of the coefficient  $\kappa$ ), preparation of the list of molecules for which computations were performed, DFT computations, processing of the results of the CCSD and DFT computations. I wrote the first version of the paper. I estimate my contribution to this work as approximately 60 %.*

Bibliometric data of articles of the scientific achievement:

|                               |               |
|-------------------------------|---------------|
| Total number of publications: | <b>7</b>      |
| Total impact factor:          | <b>21.144</b> |
| Sum of MNiSW points:          | <b>230</b>    |

## **D. The aim of the above mentioned papers and description of the scientific achievement**

### **D.1. Introduction**

Nuclear magnetic resonance (NMR) spectroscopy investigates the interactions of the nuclear dipole moments in the presence, at least for the typical studies on the structure and physicochemical properties of molecules, of a strong magnetic field of the magnitude of several teslas. This experimental approach has been successfully applied, over the several years, in studies aiming to determine the atom connectivity and the three-dimensional structures of molecules in the liquid phase, which allow us to deduce biochemical properties in an environment similar to *in vivo* conditions [1]. However, more subtle structural properties, such as the molecular chirality, may be inferred from the results of NMR spectroscopy only in an indirect specific to a given group of chemical compounds way [2]. The range of information obtained from NMR studies could be significantly extended if the presence of an external perturbation of the system under consideration is permitted, particularly that induced by an electric field. In this case, according to theoretical predictions discussed further in detail in this work, the blindness of NMR spectroscopy to chirality molecular is lifted and the postulated effects provide a novel method to determine the molecular structural parameters.

From the seven articles, which are discussed in this dissertation, papers **H1-H4** introduce five new NMR effects. In the paper **H5**, a promising experimental setup is described, which could be used for the detection of two other effects predicted earlier as well as the theory necessary for building the setup. The results of the quantum chemistry computations of pseudoscalars determining the magnitudes of the postulated effects, those analyzed in the papers **H3** and **H5**, are presented in articles **H6** and **H7**, respectively. After a brief introduction to the mathematical formalism used in this work, each of these effects is described in detail, *i.e.*, the proposed experimental protocol for observation of the effect, estimation of the magnitude of the anticipated signal, and the significance of the effect for the determination of the molecular structure.

### **D.2. Significance of the predicted effects for enantiomers discrimination**

The existing methods of chirality determination have attracted noticeable interest. Therefore, several new methods have been proposed [3-5]. However, none of the methods developed thus far are widely used. The indirect methods commonly used in chemical applications (*vide infra*) are based on the concept that a chiral environment has different

effects on the enantiomers of a given chemical compound. Direct methods are polarimetry and circular dichroism. However, note that, in practice, the use of polarimetry for the studies of new compounds is rather limited, as the rotation angle for the compound obtained for the first time is unknown. This technique is used instead for the determination of the enantiomeric excess. More information can be obtained from vibrational optical activity, but this is only practical for small molecules and non-aqueous samples. Similarly, Raman optical activity is not a widely used technique as the interpretation of its spectra is demanding.

Enantiomers are routinely discriminated using chromatographic separation with a chiral stationary phase. The limitation of this method is the choice of the stationary phase for each of the studied systems. To a certain extent one can anticipate the appropriate stationary phase from the chemical similarity between compounds, but in practice, usually, the tedious trial-and-error method is applied, for example, the use of 10–15 chromatographic columns to find the best stationary phase. Finding a suitable stationary phase requires a considerable large amount of the compound (usually approx. 1 g); therefore, a scaling-up reaction is necessary, which particularly for the multi-step linear synthesis is time-consuming. Therefore, chromatography is useful for separating enantiomers, but has limited use for determining structure.

One infers about chirality from the NMR spectra of diastereomers obtained using chiral derivatizing agents, chiral solvents [6], complexes with chiral molecules [2], and chiral carrageenan gels [7]. These indirect methods are specific to a particular target molecule or a class of molecules. They are also time-consuming, and in the case of derivatization, the recovery of the chiral analyte is difficult. Therefore, the exploration of other direct ways to solve the issue of chirality determination by using NMR spectroscopy could be very advantageous. The introduction of these methods may permit the determination of interatomic connectivity, the three-dimensional structure, and chirality of a molecule, and therefore, fully characterize the structure of the molecule by using the measurements performed using only one type of spectroscopy. This is particularly important in the case of *in situ* biomolecular studies and the quality control of medical products. The following two examples illustrate this point. One enantiomer of thalidomide is a teratogen (causes malformation of fetus' limbs), while the other enantiomer has a therapeutic effect (first used against morning sickness in pregnant women, and currently used as an immunomodulatory drug). Therefore, efficient methods for chiral discrimination are of considerable importance

for medical and pharmaceutical studies, and the Food and Drug Administration now requires the monitoring of the handedness of a chiral drug molecule throughout the entire production process. The second example is the phenomenal ability of the human nose to discriminate between some chiral molecules. For instance, (*S*)-carvone is primarily responsible for caraway's distinct odor, and (*R*)-carvone is mainly responsible for the smell of spearmint. Several other examples can be found in Ref. [8]. Therefore, efficient methods of chiral discrimination can have some long-term effects on the quality control of industrial processes, such as food processing.

### D.3. Irreducible spherical decomposition of a tensor

The tensor analysis is frequently referred to in the following text; therefore, let us briefly summarize the relevant tensor properties from the viewpoint of this work. Any second-rank tensor  $\mathcal{A}$  (represented by a  $3 \times 3$  matrix for the tensors considered here) can be decomposed into a sum of its components of at most the second rank [9],

$$\mathcal{A} = \mathcal{A}^{iso} \mathbf{1} + \mathcal{A}^{anti} + \mathcal{A}^{sym}, \quad (1)$$

where  $\mathbf{1}$  is the unity tensor,  $\mathcal{A}^{iso} = \frac{1}{3}\text{Tr}(\mathcal{A})$  is the isotropic part,  $\mathcal{A}^{anti} = \frac{1}{2}(\mathcal{A} - \mathcal{A}^T)$  is the antisymmetric part, and  $\mathcal{A}^{sym} = \frac{1}{2}(\mathcal{A} + \mathcal{A}^T) - \mathcal{A}^{iso} \mathbf{1}$  is the traceless symmetric part of the tensor  $\mathcal{A}$ . The antisymmetric part of the tensor  $\mathcal{A}$  represented as a vector can be expressed as follows [10]:

$$\mathcal{A}^* = \frac{1}{2}(\mathcal{A}_{23} - \mathcal{A}_{32}, \mathcal{A}_{31} - \mathcal{A}_{13}, \mathcal{A}_{12} - \mathcal{A}_{21}). \quad (2)$$

The ranks of the isotropic, antisymmetric, and traceless symmetric parts of tensor  $\mathcal{A}$  are zero, one, and two, respectively.

Usually, only the isotropic parts, mostly in the liquid-state NMR, and the symmetric parts of the relevant tensors, mainly in the solid-state NMR, are experimentally studied [11]. However, as will be shown, the presence of the antisymmetric component induces interesting phenomena in the electric field.

### D.4. Hamiltonian of a spin system perturbed by an electric field

The averaged-over-the-sample Hamiltonian of a spin system consisting of spins  $I_1, I_2, \dots, I_n$  that is placed in the static magnetic field  $\mathbf{B}$  is

$$\hat{\mathcal{H}}_B = \hat{\mathcal{H}}_{CS} + \hat{\mathcal{H}}_D + \hat{\mathcal{H}}_J. \quad (3)$$

In the following text, it is assumed that all of the nuclei of the spin system have the spin quantum number  $\frac{1}{2}$ . The contributions to the Hamiltonian  $\hat{\mathcal{H}}_B$  ordered according to their magnitude for the case of the strong magnetic field  $\mathbf{B}$  are as follows. The Hamiltonian  $\hat{\mathcal{H}}_{CS}$  describes the interaction of the spins with the magnetic field at the position of the nucleus; *i.e.*, the field is reduced by the nuclear magnetic shielding caused by the electrons of the molecule. This interaction describes the nuclear magnetic shielding tensor  $\sigma$ . The Hamiltonian  $\hat{\mathcal{H}}_D$  is an energy of the direct dipole-dipole interaction between the spins  $I_i$  and  $I_j$  ( $i \neq j$ ) given by the direct spin-spin coupling tensor  $\mathbf{D}_{I_i I_j}$ . The Hamiltonian  $\hat{\mathcal{H}}_J$  describes the indirect dipole-dipole interaction between the spin  $I_i$  and the spin  $I_j$  ( $i \neq j$ ), which is mediated by the electrons of the molecule; it is described by the indirect spin-spin coupling tensor  $\mathbf{J}_{I_i I_j}$ . These Hamiltonians, written using the decomposition from Eq. (1), are as follows:

$$\hat{\mathcal{H}}_{CS}/\hbar = -\sum_{i=1}^n \gamma_{I_i} \left( \sigma_{I_i}^{iso} \hat{\mathbf{I}}_i \cdot \mathbf{B} + \sigma_{I_i}^* \cdot (\mathbf{B} \times \hat{\mathbf{I}}_i) + \hat{\mathbf{I}}_i \sigma_{I_i}^{sym} \mathbf{B} \right), \quad (4)$$

$$\hat{\mathcal{H}}_D/\hbar = \sum_{i=1}^n \sum_{\substack{j=1 \\ j>i}}^n \hat{\mathbf{I}}_i \mathbf{D}_{I_i I_j}^{sym} \hat{\mathbf{I}}_j, \quad (5)$$

$$\hat{\mathcal{H}}_J/\hbar = 2\pi \sum_{i=1}^n \sum_{\substack{j=1 \\ j>i}}^n \left( J_{I_i I_j}^{iso} \hat{\mathbf{I}}_i \cdot \hat{\mathbf{I}}_j + \mathbf{J}_{I_i I_j}^* \cdot (\hat{\mathbf{I}}_i \times \hat{\mathbf{I}}_j) + \hat{\mathbf{I}}_i \mathbf{J}_{I_i I_j}^{sym} \hat{\mathbf{I}}_j \right), \quad (6)$$

where  $\gamma_{I_i}$  is the gyromagnetic ratio of the  $i^{th}$  nucleus. In Eqs. (4)–(6), it is assumed that the orientation of the molecule is fixed with respect to the laboratory frame of reference. The influence of the molecular tumbling in the liquid phase is taken into account in Sec. D.6.

Suppose that the sample is a liquid and it consists of molecules, which have the permanent electric dipole moment  $\boldsymbol{\mu}^e$ . The energy of a molecule that has the electric dipole  $\boldsymbol{\mu}^e$  and it is placed in an electric field  $\mathbf{E}$  is  $-\boldsymbol{\mu}^e \cdot \mathbf{E}$ . Therefore, using the Boltzmann average over an ensemble of molecules placed in the electric field, we find that the Hamiltonian of the spin system, which is perturbed by the electric field, is [H1]:

$$\hat{\mathcal{H}}_{EB} \approx \left( 1 - \frac{\boldsymbol{\mu}^e \cdot \mathbf{E}}{k_B T} \right) \hat{\mathcal{H}}_B, \quad (7)$$

where  $k_B$  is the Boltzmann's constant and  $T$  is the temperature. The  $\mathbf{E}$  field and the  $\mathbf{B}$  field in Eq. (7) are the local (microscopic) fields and they may differ from those applied externally in the experiment. These differences may be considerably more pronounced for the electric

field than for the magnetic field as for a typical diamagnetic sample, the relative permittivity is greater than the relative permeability.

The condition that the molecule bears a permanent electric dipole moment is not necessary for the existence of the predicted NMR effects induced by the electric field  $\mathbf{E}$ . However, for molecules, that do not meet this condition, the amplitudes of the expected effects are too small for practical usage; thus, their discussion will be omitted [H1, H4]. In the case of the lack of a permanent dipole moment, the effects depend on the polarizability of the magnetic shielding tensor  $\sigma_{ijk}^1$  and the polarizability of the indirect spin-spin coupling tensor  $J_{ijk}^1$ , which are the linear terms in the power series expansion of the tensors  $\sigma$  and  $\mathbf{J}$  as a function of the electric field  $\mathbf{E}$ , *i.e.*,

$$\sigma_{ij}(E) = \sigma_{ij}^0 + \sigma_{ijk}^1 E_k + \dots, \quad (8)$$

$$J_{ij}(E) = J_{ij}^0 + J_{ijk}^1 E_k + \dots. \quad (9)$$

Analogous effects to those described further (*i.e.*, effects **E1–E7**) are present if  $\mu^e = 0$  and they are found by the substitutions  $\sigma_{ij}^0 \mu_k^e \rightarrow \sigma_{ijk}^1$  and  $J_{ij}^0 \mu_k^e \rightarrow J_{ijk}^1$ . For the sake of brevity, the index zero for the unperturbed tensors  $\sigma$  and  $\mathbf{J}$  is omitted in the following text.

#### **D.5. Relationship between molecular chirality and NMR phenomena involving the electric field**

The parity non-conservation does not have the influence on NMR spectra measured by the currently used NMR spectrometers [12, 13]. Consequently, one assumes that the Hamiltonian  $\hat{\mathcal{H}}_B$  is even under the inversion through a point. Therefore, one cannot directly discriminate between the enantiomers by NMR spectroscopy unless the molecule is transformed into a diastereomer (*e.g.*, via the Mosher's method [14]) or a chiral environment is present. This limitation is lifted if an odd under inversion electric field operator is involved in the Hamiltonian [15, H5]. In this case, some contributions to the Hamiltonian  $\hat{\mathcal{H}}_{EB}$  (*vide infra*) change their sign under the inversion, which may be used for a direct discrimination between the enantiomers. All of these effects generate NMR signals of the opposite phase (*i.e.*, phase-shifted by 180°) for the enantiomers of a given molecule. Note that the linear in the electric field effects are chirality-sensitive and they vanish for an achiral sample. In contrast, the quadratic effects are present in the achiral and the chiral samples.

### D.6. Mathematical framework used to find the effects induced by the $E$ field

The time evolution of the spin system under the influence of the externally applied electric field  $E$  is given by the solution of the Liouville von Neumann equation,

$$\frac{\partial \rho(t)}{\partial t} = -i \left[ \frac{\hat{\mathcal{H}}_{EB}(t)}{\hbar}, \rho(t) \right], \quad (10)$$

where  $\rho(t)$  is the density matrix of the spins ensemble. To find tractable analytical solutions of Eq. (10), averaged over the ensemble of tumbling molecules, it is convenient to use the second-order perturbation theory. This approach is used in the Bloch-Redfield-Wangsness theory [16, 17]. For the considered case, *i.e.*, isotropic diffusion, the changes of the density matrix  $\rho(t)$  in time may be evaluated using the irreducible spherical tensor decomposition without the need of averaging over molecular orientations explicitly. In the standard case, *i.e.*, without the electric field, this approach was used in Ref. [18]. If the coefficients of the obtained relaxation matrix are time-dependent, *i.e.*, in the case of the modulated electric field, then the equation is further approximated by transforming the reference frame to a frame that rotates around the  $z$ -axis with the spin precession frequency of each spin, next expansion of the obtained fundamental matrix in the Floquet-Magnus series, and truncation of the series after the few first terms [19].

The number of irreducible spherical components of the Hamiltonian  $\hat{\mathcal{H}}_{EB}$  is larger than 30, even for the two-spin system, which gives at least a thousand of interactions described by the tensors. Therefore, a careful selection of the desired interactions is mandatory. This selection is based on the following three criteria: (i) the amplitude of the effect is sufficiently large for the detection in the magnetic and electric fields of the strengths accessible in the currently used experimental equipment, (ii) an appropriately designed experiment allows the separation of the effect from other simultaneously present effects, (iii) an experimental observation of the effect reveals interesting information about the molecular structure for chemists and physicists.

### D.7. Predicted effect induced by an electric field $E$

In the following text, we assumed that the sample is a liquid and the molecules tumble considerably faster than the variation of the electric field in time. The postulated effects are grouped with respect to their sensitivity to the molecular chirality and the size of the spins

system required for their observation. The specific conditions for each of the predicted effects are as follows.

***Effects observable for a single spin placed in any molecule, not necessarily chiral***

D.7.1. Transverse relaxation rate induced by the isotropic nuclear magnetic shielding [H1]

*Description of effect E1*

The nuclear shielding tensor  $\sigma$  perturbed by the electric field  $\mathbf{E}$  has a contribution that transforms like a vector and depends on the isotropic nuclear magnetic shielding  $\sigma_{\text{iso}}$ . This contribution is

$$\frac{\sigma_{\text{iso}}}{k_B T} \hbar \gamma_N (\boldsymbol{\mu}^e \cdot \mathbf{E}) (\hat{\mathbf{I}} \cdot \mathbf{B}_0), \quad (11)$$

where  $\mathbf{B}_0$  is the main static field of the NMR spectrometer. The transverse, but not the longitudinal, relaxation rate is affected by the presence of this contribution to the Hamiltonian  $\hat{\mathcal{H}}_{EB}$ . The nuclear relaxation rate, which depends on the isotropic shielding, is

$$\frac{1}{T_2} = \frac{1}{3} \left( \frac{\mu^e E}{k_B T} \right)^2 (\gamma_N B_0)^2 \sigma_{\text{iso}}^2 \tau_1, \quad (12)$$

where  $\tau_1$  is the first rank rotational diffusion correlation time.

*Proposed experimental protocol*

The effect **E1** may be experimentally observed by measuring of the transverse nuclear relaxation rate determined by the Carr-Purcell-Meiboom-Gill pulse sequence [20, 21] with and without the electric field  $\mathbf{E}$ . For an axially symmetric shielding tensor (*i.e.*, with two principal components equal to each other) the relative increase in the relaxation rate under the influence of the electric field is

$$\frac{\frac{1}{T_2} - \frac{1}{T_2^{E=0}}}{\frac{1}{T_2^{E=0}}} = \left( \frac{\mu^e E}{k_B T} \right)^2 \left( \frac{45}{7} \left( \frac{\sigma_{\text{iso}}}{\Delta} \right)^2 + \frac{1}{2} \right), \quad (13)$$

where the angle between the electric and the magnetic fields is the magic angle, *i.e.*,  $\theta_M = \arccos(1/\sqrt{3}) \approx 54.7^\circ$ . This angle minimizes the unwanted contributions proportional to the anisotropy of the shielding tensor  $\Delta = \sigma_{33} - (\sigma_{11} + \sigma_{22})/2$ .

*Estimation of effect magnitude*

A favorable sample for the experiment is a molecule that possesses a nucleus having large isotropic shielding and the small anisotropy of a shielding tensor, as the anisotropy inherently contributes to the total transverse relaxation rate even without the electric field. This criterion is fulfilled by the  $^{205}\text{Tl}$  nucleus in the cluster  $\text{Pt}(\text{CN})_6\text{Tl}$ . Relativistic density functional theory computations indicate that the isotropic shielding of the nucleus  $^{205}\text{Tl}$  in  $\text{Pt}(\text{CN})_6\text{Tl}$  exceeds 12000 ppm, and the anisotropy is at least 10 times smaller than the isotropic shielding. Thus, the electric field  $\mathbf{E}$  of the strength 5 kV/mm induces twice faster transverse nuclear relaxation than that induced in the case when the electric field is not applied.

*Significance of the effect*

A possible application of **E1** is the determination of the isotropic nuclear shielding for heavy nuclei, which usually have considerably large isotropic shielding. For these nuclei, the uncertainty of an isotropic shielding is up to several hundred parts per million, since for heavy nuclei, the magnetic moments are known with precision to be approximately two or three orders of magnitude lower than for those for the light nuclei [22]. The experimental methods for the measurement of nuclear magnetic moments are reviewed in Ref. [23].

D.7.2. Transverse component of the magnetization induced by the electric field [H2]*Description of the effect E2*

In the absence of the externally applied electric field  $\mathbf{E}$ , the longitudinal and transverse nuclear relaxation processes are independent of each other. However, the introduction of the electric field  $\mathbf{E}$  results in the off-diagonal elements in the Bloch equation,

$$\frac{d\mathbf{M}(t)}{dt} = \gamma_N \mathbf{M}(t) \times \mathbf{B} - \gamma_N^2 \left( (\mathbf{B} \cdot \mathbf{E}) |\mathbf{B} \times \mathbf{E}| \begin{pmatrix} 0 & 0 & r \\ 0 & 0 & 0 \\ r & 0 & 0 \end{pmatrix} + B^2 \begin{pmatrix} t_2 & 0 & 0 \\ 0 & t_2 & 0 \\ 0 & 0 & t_1 \end{pmatrix} \right) (\mathbf{M}(t) - \mathbf{M}_{eq}) \tau_1, \quad (14)$$

where  $\mathbf{M}$  is the nuclear magnetization,  $T_1^{-1} = \gamma_N^2 B^2 t_1 \tau_1$  and  $T_2^{-1} = \gamma_N^2 B^2 t_2 \tau_1$  are the longitudinal and the transverse relaxation rates, respectively;  $t_1 = \frac{2}{3} (\sigma^*)^2 + \frac{2}{45} \Delta^2$  and  $t_2 = \frac{1}{3} (\sigma^*)^2 + \frac{7}{135} \Delta^2$ . In Eq. (14), the other contributions to the relaxation

matrix, which are induced by the electric field, are neglected as they contribute only to the diagonal of the matrix. The coefficient  $r$  for an axially symmetric nuclear shielding tensor  $\sigma$  is

$$r = \frac{3}{2}(1 + 3 \cos 2\theta) \left(\frac{\mu^e}{k_B T}\right)^2 \Delta(\Delta + 7\sigma_{\text{iso}}), \quad (15)$$

where  $\theta$  is the angle between the permanent electric dipole moment  $\mu^e$  of the molecule and the z-axis of the principal axis system of the tensor  $\sigma$ .

#### Proposed experimental protocol

The experimental protocol is shown in Fig. 1. Initially, the nuclear magnetization is in thermodynamic equilibrium,  $\langle I_z \rangle_0 = \hbar\omega/(4k_B T)$ , where  $\omega$  is the nuclear spin precession frequency in the magnetic field  $\mathbf{B}_0$ . When the nuclear magnetization returns from the direction that is opposite to the magnetic field, the electric field  $\mathbf{E}$  induces the transverse component of the magnetization, which is not present without the electric field. To increase the magnitude of the effect,  $\mathbf{E}$  is not static but oscillates at the half of the spin precession frequency (Fig. 1A). This field is created by the capacitor tilted by  $45^\circ$  with respect to the field  $\mathbf{B}_0$ , i.e.,  $\mathbf{E} = E_1 \cos(\omega t)(\hat{x} + \hat{z})$  (Fig. 1B). The optimal time for the application of the electric field is equal to the longitudinal relaxation time of the sample measured in absence of the electric field  $\mathbf{E}$ , i.e.,  $\tau = T_1$  (Fig. 1C). Next, the induced transverse component of the magnetization is detected by a coil (not shown in Fig. 1).

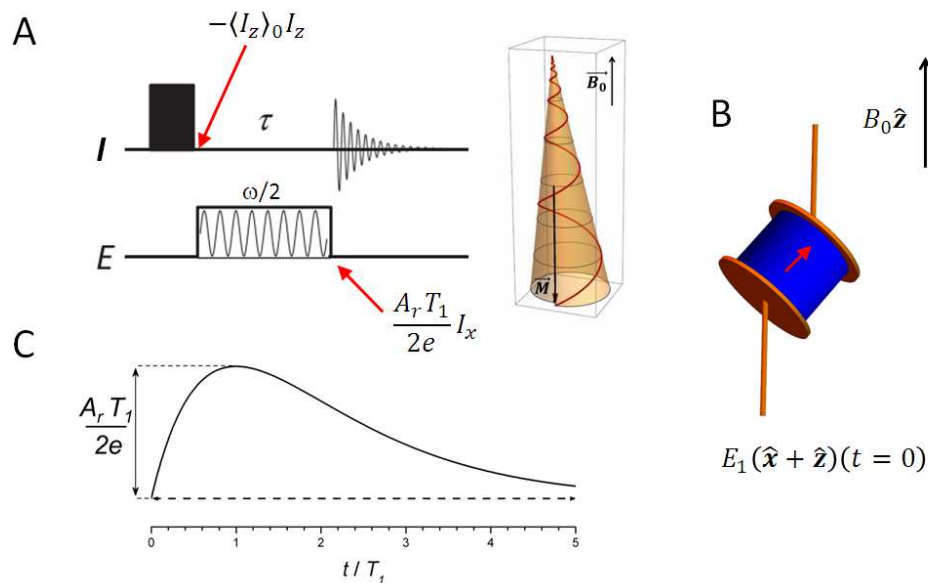


Fig. 1. Experimental protocol for observation of the effect **E2**. See details in the text.

*Estimation of effect magnitude*

Assuming that  $\tau_1 = 10$  ps,  $B_0 = 10$  T, and  $E = 5$  kV/mm, we find that the estimated amplitude of the effect **E2** for the  $^{195}\text{Pt}$  nucleus in the cisplatin molecule is 10 mHz, which corresponds to a signal approximately four orders of magnitude smaller than that obtained from the same sample in the thermodynamic equilibrium after the application of a  $90^\circ$  pulse without the electric field **E**.

*Significance of the effect*

By determining of the angle  $\theta$ , one can find the relative orientation of the moiety containing the nucleus with respect to the permanent electric dipole moment  $\mu^e$  of the molecule. The required components of the shielding tensor  $\sigma$  may be found independently, e.g., from solid-state magic angle spinning experiments and application of a Herzfeld-Berger analysis [24].

***Effects observable for a single spin placed in a chiral molecule; thus, vanishing for non-chiral molecules***

D.7.3. Electric polarization induced by antisymmetry of shielding tensor [H5, H7]*Description of the effect E3*

This effect was predicted by Buckingham [15, 25] and Buckingham and Fischer [26]. The nuclear magnetization **M**, which precesses in the magnetic field **B**<sub>0</sub>, generates in a liquid sample containing the chiral molecules with non-vanishing permanent electric dipole moment  $\mu^e$ , the chirality-sensitive electric polarization

$$\mathbf{P}(t) = \sigma_c \mathbf{B}_0 \times \mathbf{M}(t), \quad (16)$$

where the pseudoscalar characterizing its amplitude is

$$\sigma_c = \frac{\mu^e \cdot \sigma^*}{3k_B T}. \quad (17)$$

The pseudoscalar  $\sigma_c$  has the opposite sign for the enantiomers and vanishes if the molecule is not chiral.

*Proposed experimental protocol*

The induced electric polarization  $\mathbf{P}$  is detected by a capacitor. Any capacitor used at radiofrequencies has some parasitic inductance; *i.e.*, it partially acts as a coil and, thus, it can be excited by the variation of the magnetic field in time. Therefore, it generates an unwanted signal of the nuclear magnetization  $\mathbf{M}$ , which is the same for both enantiomers [H5]. The expected signal  $\mathcal{S}(P)$  of the electric polarization  $\mathbf{P}$  is considerably weaker than the signal  $\mathcal{S}(M)$  of the magnetization  $\mathbf{M}$ . The ratio of these two signals is [H7]

$$\frac{\mathcal{S}(P)}{\mathcal{S}(M)} = \kappa^{-1} \left( \frac{cP}{M} \right). \quad (18)$$

The ratio  $cP/M$  is smaller than  $10^{-4}$  for diamagnetic samples; thus, it is important to use an experimental set up that has a low value of coefficient  $\kappa$ . Thus, one can use the loop-gap resonator, which allows the suppression of the unwanted signal of the precessing nuclear magnetization.

The experimental protocol for effect **E3** is shown in Fig 2. Initially, the magnetization  $\mathbf{M}$  is rotated from its equilibrium position along the direction of the magnetic field  $\mathbf{B}_0$  to the  $xy$ -plane and then precesses with the frequency  $\omega$  (Fig. 2A). Its precession induces the chirality-sensitive electric polarization  $\mathbf{P}$ , which in the rotating reference frame with the frequency  $\omega$ , is along the  $x$ -axis (Fig. 2B). For a sample placed between the plates of the resonator, the signal  $\mathcal{S}(P)$  of polarization  $\mathbf{P}$  is opposite to that for enantiomers (shown arbitrarily as a positive peak for the (*R*)-enantiomer and a negative peak for the (*S*)-enantiomer). If the symmetry of the resonator is preserved, then the unwanted signal  $\mathcal{S}(M)$  of the magnetization  $\mathbf{M}$  integrated over the sample is zero (Fig. 2C). See Ref. [H5] for more details about the resonator.

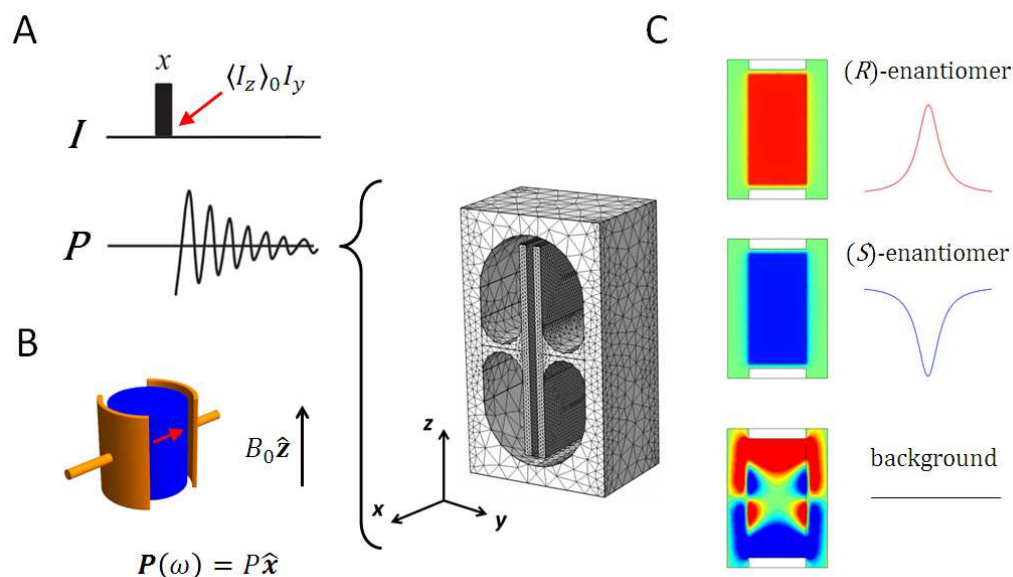


Fig. 2. Experimental protocol for observation of the effect **E3**. See details in the text.

#### *Estimation of effect magnitude*

Favorable samples for this experiment are the derivatives of cyclopropane (e.g., 1,3-diphenyl-2-fluoro-3-trifluoromethylcyclopropene) and light alcohols (e.g., 1,1,1-trifluoropropan-2-ol), which contain the fluorine nucleus. The latter are more convenient as they are stable at room temperature. The estimated magnitude of the chirality-sensitive electric polarization for these samples is  $P = 100 \text{ aC/m}^2$  at the magnetic field of the strength  $B_0 = 10 \text{ T}$ .

#### *Significance of the effect*

This is one of the strongest predicted effects. The main advantage of the observation of effect **E3** is that the sample is not perturbed by the dielectric heating. If the sign of the product  $\mu^e \cdot \sigma^*$  is known from the quantum chemistry computations, then the experimental determination of the sign of the signal  $\mathcal{S}(P)$  allows one to not only distinguish between enantiomers but also determine the absolute configuration of the molecule.

D.7.4. Magnetization induced by antisymmetry of shielding tensor [H5, H7]*Description of effect E4*

The chirality-sensitive contribution to the Hamiltonian  $\hat{\mathcal{H}}_{EB}$  from the nuclear shielding tensor  $\sigma$  that does not average out in the liquid phase is  $-\gamma\hbar\sigma_c(\mathbf{B} \times \hat{\mathbf{I}}) \cdot \mathbf{E}$ . Note that the mixed triple product is invariant under the cyclic permutations of its components. Therefore, the energy  $-\gamma\hbar\sigma_c(\mathbf{B} \times \hat{\mathbf{I}}) \cdot \mathbf{E}$  may be interpreted either as the energy  $\mathcal{H} = -\boldsymbol{\mu}_e^{c,\sigma} \cdot \mathbf{E}$  of the induced electric dipole moment  $\boldsymbol{\mu}_e^{c,\sigma} = \gamma\hbar\sigma_c(\mathbf{B} \times \hat{\mathbf{I}})$  in the electric field  $\mathbf{E}$  (the effect discussed in the previous section, **E3**), or the energy  $\mathcal{H} = -\boldsymbol{\mu}_m^{c,\sigma} \cdot \mathbf{B}$  of the induced magnetic dipole moment  $\boldsymbol{\mu}_m^{c,\sigma} = \gamma\hbar\sigma_c(\hat{\mathbf{I}} \times \mathbf{E})$  placed in the magnetic field (the effect described in this section, **E4**). This effect was described by Buckingham and Fischer [26]; more details are given in Refs. [27] and [28]. For this contribution, the equation describing the dynamics of the magnetization in the electric field  $\mathbf{E}$  and the magnetic field  $\mathbf{B}$  is

$$\frac{d\mathbf{M}(t)}{dt} = \gamma_N \mathbf{M}(t) \times (\mathbf{B} + \sigma_c \mathbf{B} \times \mathbf{E}) - \gamma_N^2 B^2 \begin{pmatrix} t_2 & 0 & 0 \\ 0 & t_2 & 0 \\ 0 & 0 & t_1 \end{pmatrix} (\mathbf{M}(t) - \mathbf{M}_{eq}) \tau_1, \quad (19)$$

In Eq. (19), the influence of the electric field  $\mathbf{E}$  on the relaxation processes is neglected.

*Proposed experimental protocol*

Even for the sample placed in the electric field of the strength  $E = 1$  kV/mm for which the pseudoscalar  $\sigma_c$  is 1 fm/V, the term  $\sigma_c E$  is considerably smaller than unity; thus, the angle of the rotation of the nuclear magnetization is a few orders of magnitude smaller than in the case of the time-dependent electric field in comparison with the magnetic field varying in time. Let us assume that at a given point in the sample, the electric field is  $\mathbf{E}_1 = E_1 \sin(\omega t) \hat{\mathbf{y}}$ . This field according to the Maxwell equations generates the magnetic field oscillating at the same frequency,  $\mathbf{B}_1 = B_1 \cos(\omega t) \hat{\mathbf{x}}$  as that of the field  $\mathbf{E}_1$ . For the strong magnetic fields, the component of the magnetic field  $\mathbf{B}_1$ , which has the same direction as the magnetic field  $\mathbf{B}_0$ , practically does not affect the state of the nuclear spins [28, H5]. Taking into account the nuclear relaxation processes, one finds that the steady state of

the nuclear magnetization obtained after the application of the electric field for a long period  $\tau$  (in practice, it is sufficient to fulfill the condition  $\tau > 3T_1$ ) is

$$\frac{M_{t \rightarrow \infty}}{M_{\text{eq}}} = \frac{1}{1 + T_1 T_2 \Omega^2} (\pm T_2 \omega_E, -T_2 \omega_B, 1), \quad (20)$$

where  $T_1$  and  $T_2$  are the longitudinal and the transverse relaxation times, respectively. In Eq. (20), the frequencies of the nuclear magnetization nutation caused by the electric and magnetic fields are  $\omega_E = |\sigma_c| E_1 \gamma B_0 / 2$  and  $\omega_B = \gamma B_1 / 2$ . The other quantities are defined as follows

$$\Omega = \omega_{E_y} \sqrt{1 + \left(\frac{\kappa}{\kappa_N}\right)^2}, \quad (21)$$

where the ratio  $\kappa = cB_1/E_1$  depends on the electric and magnetic fields generated by the capacitor (resonator) used in the experiment; the ratio  $\kappa_N = \sigma_c c B_0$  ( $c$  is the speed of light and  $B_0$  is the main magnetic field of the NMR spectrometer) depends on the studied sample.

The details of the experimental protocol are shown in Fig. 3. The electric field  $\mathbf{E}_1$  that oscillates with the spin precession frequency  $\omega$  for the duration  $\tau > 3T_1$  rotates the nuclear magnetization (Fig. 3A). The electric field  $\mathbf{E}_1$  may be generated by a capacitor; however, the oscillating-in-time  $\mathbf{B}_1$  field saturates the magnetization and decreases the amplitude of the chirality-sensitive signals (more details are given in [H5]). Therefore, a sufficiently effective suppression of the unwanted magnetic  $\mathbf{B}_1$  requires a dedicated resonator. The resonator consists of a capacitor modified by adding two loops (*i.e.*, loop-gap resonator). The magnetic field generated by these loops cancels the transverse component of the magnetic field generated by the capacitor, and the resultant magnetic field is oriented in the same direction as the field  $\mathbf{B}_0$  of the NMR spectrometer. The volume of the sample placed in the central point between plates in which unwanted magnetization excitation does not saturate the magnetization, marked by the red color ( $\kappa < 10^{-5}$ ), is sufficiently large for generating a signal of the order of 10 % of the signal generated in the standard NMR experiment (Fig. 3B). The obtained signals of the enantiomers have different phases; *i.e.*, contribute to the spectrum as the positive and the negative peaks. The positive peak is arbitrarily attributed to the (*R*)-enantiomer (Fig. 3C).

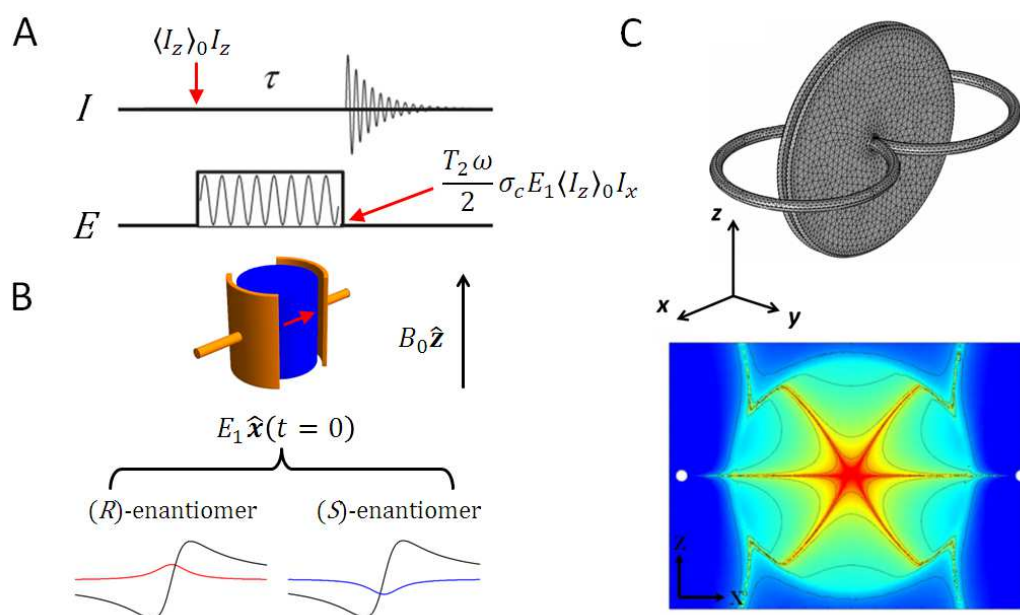


Fig. 3. Experimental protocol for observation of the effect **E4**. See details in the text.

#### Estimation of effect magnitude

The favorable samples for the effect **E4** are the same as those for the effect **E3**. Taking into account the possible imperfections of the fabrication of the resonator, the estimated chirality-induced NMR signal that accounts for 1–5 % of the standard achiral NMR signal is predicted for the electric field of the strength  $E = 10$  V/mm and the magnetic field  $B_0 = 10$  T.

#### Significance of the effect

Similarly to the effect **E3**, the effect **E4** allows one to discriminate between enantiomers and it has one of the largest amplitudes of the chirality-sensitive effects described here. The main limitation for its detection is the suppression of the unwanted magnetic field which is generated by the oscillating-in-time electric field and convection in the sample caused by the dielectric heating by the **E** field.

***Effects observable in a two-spin system specific to chiral molecules, thus, vanishing for non-chiral molecules***

D.7.5. Electric polarization induced by antisymmetric part of indirect spin-spin coupling [H3, H6]

*Description of effect E5*

A liquid sample containing chiral molecules, which has the non-vanishing permanent electric dipole moment  $\mu^e$  and the two-spin system (spins  $I$  and  $S$ ) interacting by the indirect spin–spin coupling, has the following chirality-sensitive electric polarization [H3]

$$\mathbf{P} = -\mathcal{N}hJ_{IS}^c \mathbf{I} \times \mathbf{S}, \quad (22)$$

where  $\mathcal{N}$  is the density of spins per unit volume and

$$J_{IS}^c = \frac{\mu^e \cdot J_{IS}^*}{k_B T}. \quad (23)$$

The pseudoscalar  $J_{IS}^c$  has the opposite sign for the enantiomers and vanishes if the molecule is not chiral.

*Proposed experimental protocol*

The experimental protocol for the effect **E5** is shown in Fig. 4. In the first step, the desired quantum state of the two-spin system is obtained using the modified insensitive nuclei enhanced by polarization transfer (INEPT) pulse sequence (Fig. 4A). In the pulse sequence shown in this figure and Figs. 5 and 6, the delay  $\tau'$  is  $1/(4J_{IS}^{iso})$ . Then, the obtained state, which is described by the density matrix  $\rho$ , generates an oscillating-in-time electric polarization  $\mathbf{P}$  at the sum frequency  $\omega_I + \omega_S$ . Depending on the enantiomers, the induced electric polarization  $\mathbf{P}$  has a parallel or an antiparallel direction to the field  $\mathbf{B}_0$  (Fig. 4B). Note that the electric dipole moment  $\mu^e$  is a vector and the antisymmetry of the indirect spin-spin coupling tensor  $J_{IS}^*$  is a pseudovector; therefore, the sign of their scalar product is reversed for the enantiomers.

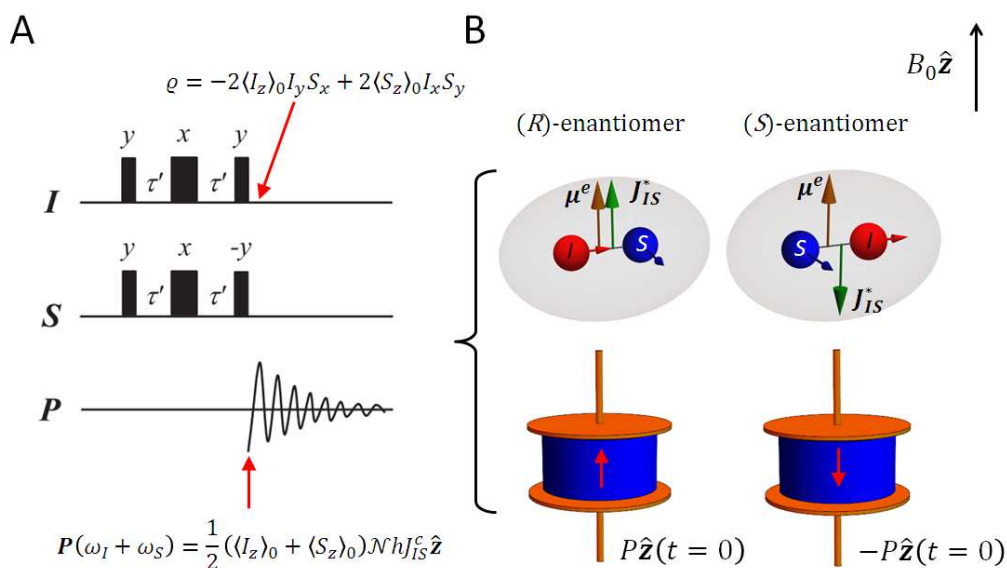


Fig. 4. Experimental protocol for observation of the effect **E5**. See details in the text.

#### Estimation of effect magnitude

The promising samples for experimental observation the effect **E5** are light fluoroalcohols (considering e.g., the two-bond fluorine-proton coupling of (1,1,1)-trifluoropropan-2-ol) and other compounds that contain fluorine (e.g., the three-bond fluorine-fluorine coupling of 1,1,1,2-tetrafluoro-2-chloroethane) [H6]. In these molecules, the pseudoscalar  $J_{\text{HF}}^e$  for the proton-fluorine spin system is of the order of 1 nHz m/V, which gives the chirality-sensitive electric polarization  $P \approx 0.1$  a/Cm<sup>2</sup> in the magnetic field of the strength  $B_0 = 10$  T. In this case, the voltage generated by this electric polarization **P** in a resonance circuit containing the capacitor has in this case the magnitude approximately five orders of magnitude smaller than that of the nuclear magnetization corresponding to the equilibrium state of the sample.

#### Significance of the effect

The effect **E5** is observable without the need to apply the electric field; thus, the sample is not affected by the dielectric heating, which may become an obstacle in the observation of the effects induced by the electric field **E**. In contrast to the effect **E3**, the induced electric polarization **P** oscillates at the sum frequency and therefore, does not overlap with the precision frequencies of the spins *I* and *S*, which simplifies the experimental setup; i.e., the detector is a parallel-plate capacitor in the radiofrequency resonant circuit.

D.7.6. Chirality-sensitive coherences induced by antisymmetric part of  $J$ -coupling tensor  
[H3, H6]

*Description of effect E6*

The effect **E5** may be interpreted as the energy  $\mathcal{H} = -\boldsymbol{\mu}_e^{cJ} \cdot \mathbf{E}$  of the induced electric dipole moment  $\boldsymbol{\mu}_e^{cJ} = \hbar J_{IS}^c \hat{\mathbf{I}} \times \hat{\mathbf{S}}$  in an electric field (see Eq. (22)). Therefore, the chirality-sensitive contribution to the Hamiltonian  $\hat{\mathcal{H}}_{EB}$  from the indirect spin-spin coupling tensor  $\mathbf{J}$  between spins  $I$  and  $S$  that does not average out in the liquid phase is  $-\hbar J_{IS}^c (\hat{\mathbf{I}} \times \hat{\mathbf{S}}) \cdot \mathbf{E}$  [H3].

*Proposed experimental protocol*

The experimental protocol for effect **E6** is shown in Fig. 5. First, the electric field oscillating at the difference frequency,  $\mathbf{E}_1 = E_1 \sin((\omega_I - \omega_S)t) \hat{\mathbf{z}}$ , excites the sample for the duration of  $\tau = T_1$ , and then, the generated chirality-dependent coherences are converted into an observable magnetization of the spin  $I$  (Fig. 5A). In the next step, the chirality-sensitive magnetization induced by the  $\mathbf{E}$  field of the capacitor is detected by the coil (not shown), generating a signal that has the opposite phase for the enantiomers (Fig. 5B). The attribution of the positive and negative peaks to the enantiomers is arbitrary.

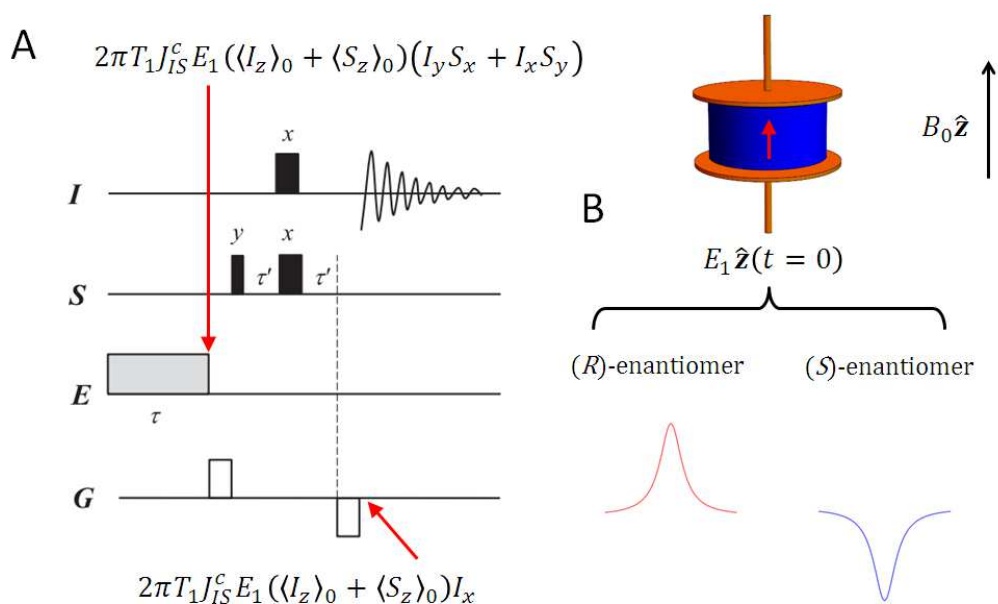


Fig. 5. Experimental protocol for observation of the effect **E6**. See details in the text.

*Estimation of effect magnitude*

The favorable samples for the observation of the effect **E6** are the same as those for the effect **E5** described in the previous section. Assume that the spin system is the pair of the proton and the fluorine nuclei, the permanent electric dipole moment of the molecule is  $\mu^e = 1$  D, and the sample is placed in the static magnetic field  $B_0 = 10$  T. Moreover, the exciting the electric field has the strength  $E_1 = 100$  V/mm, and the longitudinal relaxation time  $T_1$  is 1 s for both nuclei. Then, the estimated magnitude of the chirality-sensitive nuclear magnetization is  $10^{-4}$  of the signal of the nuclear magnetization obtained after the application of the  $90^\circ$  pulse to the sample at the thermodynamic equilibrium.

*Significance of the effect*

The application of the oscillating electric field at the difference frequency minimizes the perturbation of the system by time-dependent magnetic field generated by the  $\mathbf{E}$  field. Taking into account that the magnitude of the effect is proportional to the strength of the electric field  $E$ , and the dielectric heating is proportional to the square of the strength of the electric field, one finds that a relatively low-frequency excitation is optimal for the experiment (e.g., for the  $^1\text{H}$ - $^{19}\text{F}$  pair the difference frequency is approx. 30 MHz at the magnetic field  $B_0 = 10$  T).

D.7.7. CSA-DD relaxation mechanisms interference in electric field [H4]*Description of effect E7*

The perturbation of the interference between the dipole-dipole (DD) relaxation mechanism and the chemical shift anisotropy (CSA) relaxation mechanism by the electric field  $\mathbf{E}$  in a two-spin system, consisting of spins  $I$  and  $S$ , allows the chirality-sensitive transitions of the amplitude (described in detail in Ref. [H4]; see Fig. 2 in this reference article)

$$A^c = \sqrt{\frac{3}{2}} (\hbar\mu_0)^2 \gamma_I \gamma_S r_{IS}^{-3} \left( \frac{\mu^e E}{k_B T} \right) (\gamma_S B_0) (2\sigma^* \psi_1 + \Delta\psi_2). \quad (24)$$

In Eq. (24), it is assumed that the components of the shielding tensor  $\sigma$  of the nucleus  $I$  are considerably smaller than those for the nucleus  $S$ , and thus, they may be neglected. Moreover, the gyromagnetic ratio of the spin  $I$  is higher than that for the spin  $S$  (e.g.,  $I$  and  $S$  are  $^1\text{H}$  and  $^{13}\text{C}$ , respectively). The amplitude  $A^c$  of effect **E7** is redefined here as an inverse of that reported in Ref. [H4] to obtain a coherent description of effect **E2** predicted in Ref. [H2]. The functions  $\psi_1(\mathbf{e}_{\sigma^*}, \mathbf{e}_{\mu^e}, \mathbf{e}_b)$  and  $\psi_2(\mathbf{e}_{\Delta}, \mathbf{e}_{\mu^e}, \mathbf{e}_b)$  are defined as follows:

$$\psi_1 = \frac{1}{2} \left( (\mathbf{e}_{\sigma^*} \cdot \mathbf{e}_{\mu^e}) - 3(\mathbf{e}_b \cdot \mathbf{e}_{\mu^e})(\mathbf{e}_b \cdot \mathbf{e}_{\sigma^*}) \right), \quad (26)$$

$$\psi_2 = 2(\mathbf{e}_b \cdot \mathbf{e}_{\mu^e}) \sqrt{(\mathbf{e}_{\Delta} \times \mathbf{e}_{\mu^e})^2 (\mathbf{e}_b \times \mathbf{e}_{\mu^e})^2 - \left( (\mathbf{e}_{\Delta} \cdot \mathbf{e}_{\mu^e})(\mathbf{e}_b \cdot \mathbf{e}_{\mu^e}) - (\mathbf{e}_b \cdot \mathbf{e}_{\Delta}) \right)^2}, \quad (27)$$

where  $\mathbf{e}_{\sigma^*} = \boldsymbol{\sigma}^*/\sigma^*$ ,  $\mathbf{e}_{\mu^e} = \boldsymbol{\mu}^e/\mu^e$ , the unit vector  $\mathbf{e}_b$  is from the nucleus  $I$  to nucleus  $S$ , and the unit vector  $\mathbf{e}_{\Delta}$  is along the  $z$ -axis of the principal axis system of the symmetric part of the shielding tensor  $\sigma$ .

#### *Proposed experimental protocol*

The allowed transitions related to effect **E7** are in the populations/zero coherence block ( $M_0$ ) and the single quantum coherence block ( $M_1$ ) of the relaxation matrix of the spin system. From the viewpoint of the experimenter, the transitions in the  $M_0$  block are more convenient for detection as they require the excitation by the electric field at the difference frequency. The maximal amplitude of effect **E7** is achieved if the electric field  $\mathbf{E}$  and the field  $\mathbf{B}_0$  are parallel to each other. The experimental protocol for effect **E7** is shown in Fig. 6. At the beginning of the experiment, the initial state of the spin system,  $I_y S_x + I_x S_y$ , is created using the modified INEPT pulse sequence (Fig. 6A). Then, this state evolves under the influence of the electric field  $\mathbf{E}_1 = E_1 \sin((\omega_I - \omega_S)t) \hat{\mathbf{z}}$ . The final state induced by field  $\mathbf{E}_1$  is  $I_z$  of the amplitude  $\langle I_z \rangle_c$ , which is distinguished from the  $I_z$  component of the amplitude  $\langle I_z \rangle_{ac}$  created by the dipolar and CSA relaxation mechanism by subtracting the signal acquired with the electric field  $\mathbf{E}_1$  from that obtained without the  $\mathbf{E}_1$  field.

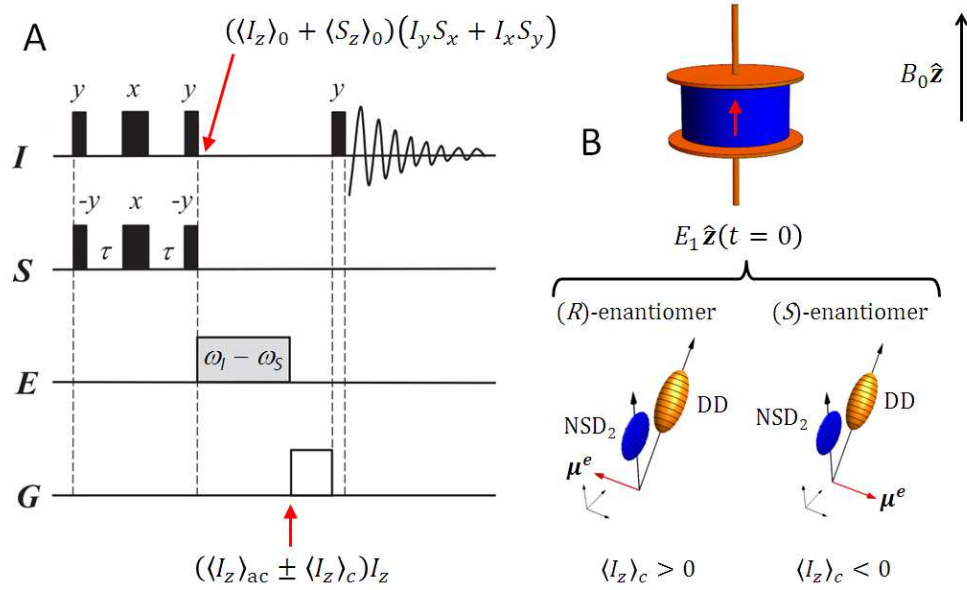


Fig. 6. Experimental protocol for observation of the effect **E7**. See details in the text.

### Estimation of effect magnitude

The magnitude of the effect depends on the strength of the field  $\mathbf{B}_0$ ,

$$T_1 A^c = \sqrt{\frac{2}{15}} \frac{\mu^e E}{k_B T} \frac{\frac{B_{\text{opt}}}{B_0}}{1 + \left(\frac{B_{\text{opt}}}{B_0}\right)^2}, \quad (28)$$

where the optimal strength of this field for the experiment is

$$B_{\text{opt}} = \frac{3\sqrt{5}}{2} (\hbar\mu_0)^2 \frac{\gamma_I \Delta_S}{r_{IS}^3}. \quad (29)$$

Let us suppose that a pair of spins are the proton and the carbon-13 separated by the typical distance of the C-H chemical bond,  $r_{\text{CH}} = 1.1 \text{ \AA}$ , and the anisotropy of the magnetic shielding of the carbon nucleus is 200 ppm, then  $B_{\text{opt}} \approx 11.75 \text{ T}$ , *i.e.*, in the range of the typical strength used in the chemical applications of NMR spectroscopy. For this optimal strength of the  $\mathbf{B}_0$  field, the permanent electric dipole moment  $\mu^e = 1 \text{ D}$ , and  $E_1 = 1 \text{ kV/mm}$  oscillating at the frequency  $\omega_{^1\text{H}} - \omega_{^{13}\text{C}}$  equal to 375 MHz, the chirality-sensitive magnetization of  $^1\text{H}$ - $^{13}\text{C}$  pair of nuclei is approximately  $5 \times 10^{-6}$  of the magnetization of the proton at the thermodynamic equilibrium.

*Significance of the effect*

In contrast to effect **E4**, which vanishes if the antisymmetric part of the nuclear shielding tensor is zero, effect **E7** even for  $\sigma^* = 0$  is non-zero (as long as  $\psi_2 \neq 0$ ); thus, it may be observable in a wider range of chiral molecules. The modulation of the electric field at the combined frequency permits the use of a simpler resonator for excitation than that required in the experiment aiming to observe the effect **E4**, *i.e.*, a parallel-plate capacitor.

## D.8. Summary

Let us briefly summarize several pieces of information, which may be obtained in the studies of the above-described effects **E1–E7**.

- (i) Effect **E1** may be used for the determination of the properties of an atomic nucleus, such as its magnetic dipole moment.
- (ii) Effects **E2–E7** are quadratic in the electric field and they are present in any, not necessarily chiral, molecule. The linear electric field effects, *i.e.*, effects **E3–E7**, are present only in the chiral samples.
- (iii) The measurements of amplitudes of effects **E2–E7** allow to determine the three-dimensional structure of the molecule. In particular, they permit finding the relative orientation of the local nuclear magnetic properties, *i.e.*, the nuclear magnetic shielding and the indirect spin-spin coupling tensors, and the permanent electric dipole moment of the molecule. Each effect depends in a different manner on the structural parameters and tensor components; thus, a combination of these effects gives a rich piece of information about the molecular structure.
- (iv) Effects **E3–E7** allow one to distinguish *directly* between enantiomers. Measurements of effects **E3–E7** combined with results of simple quantum chemistry computations permit the determination of the absolute configuration of the molecule. The quantitative measurement, *i.e.*, determination of the sign (phase) of the signals of the effects **E3–E7**, is sufficient for the assignment of the absolute configuration, which is less experimentally damaging.

The predicted effects for a single-spin and a two-spin system differ in terms to their optimal angle between the externally applied electric field **E** and the field **B<sub>0</sub>**, and the frequency of the oscillating electric field **E**, that varies in time, apart from effect **E1**. The application of the varying-in-time electric field in the case of effects **E2**, **E4**, **E6**, and **E7** increases them by at least six orders in magnitudes then the application of the static field. These factors, favorable samples for the first experiments, which were predicted from the quantum chemistry computations, and the expected signals generated by the effects are summarized in Table 1.

Table. 1 Predicted NMR effects

| Effect/<br>source<br>article | Number<br>of spins | Nuclear<br>properties         | Experimental conditions        |   | Favorable<br>sample                               | Expected<br>signal<br>magnitude* |
|------------------------------|--------------------|-------------------------------|--------------------------------|---|---|----------------------------------|
|                              |                    |                               | Angle between<br>$E$ and $B_0$ | Frequency of $P/E$<br>oscillations      |   |                                  |
| <b>E1/H1</b>                 | 1                  | $\sigma_{\text{iso}}$         | 54.7°                          | 0                                       | Pt(CN) <sub>5</sub> TI                            | $5 \times 10^{-2}$               |
| <b>E2/H2</b>                 | 1                  | $\Delta, \sigma_{\text{iso}}$ | 45°                            | $\omega_{\text{Pt}}/2$                  | Pt(NH <sub>3</sub> ) <sub>2</sub> Cl <sub>2</sub> | $5 \times 10^{-6}$               |
| <b>E3/H5,H7</b>              | 1                  | $\sigma^*$                    | N/A                            | $\omega_{\text{F}}$                     | 1,1,1-<br>trifluoro-<br>propan-2-ol               | $10^{-2}$                        |
| <b>E4/H5,H7</b>              | 1                  | $\sigma^*$                    | 90°                            | $\omega_{\text{F}}$                     |   | $5 \times 10^{-1}$               |
| <b>E5/H3,H6</b>              | 2                  | $J^*$                         | N/A                            | $\omega_{\text{H}} + \omega_{\text{F}}$ |   | $10^{-5}$                        |
| <b>E6/H3,H6</b>              | 2                  | $J^*$                         | 0°                             | $\omega_{\text{H}} - \omega_{\text{F}}$ |   | $10^{-3}$                        |
| <b>E7/H4</b>                 | 2                  | $\sigma^*, \Delta$            | 0°                             | $\omega_{\text{H}} - \omega_{\text{C}}$ | alanine   | $5 \times 10^{-6}$               |

\* The magnitude with respect to that obtained after the excitation of the sample by a 90° pulse.  
 $E = 1$  kV/mm,  $B_0 = 10$  T.

The available strength of the electric field limits the highest achievable signals of the predicted effects; therefore, a careful selection of the sample for the first set of experiments is required. The fluorine nucleus has the favorable properties as it has a high gyromagnetic ratio, large natural abundance, and notable antisymmetries of the nuclear magnetic shielding tensor and the indirect spin-spin coupling tensor in many molecules. The magnitude of the effects for the same strength of the electric field may vary depending on the particular sample; however, for a given group of chemical compounds, one can predict that their magnitudes decrease in the following series **E4**, **E1**, and **E3** > **E6** > **E5**, **E2** and **E7**. The general requirements for the experimental setup for a molecule with the permanent electric dipole moment of  $\mu^e = 1$  D, are a magnetic field  $B_0$  of the order of 10 T and an electric field  $E = 0.1$ – $1$  kV/mm, which for favorable samples shown in Table 1 (e.g., fluorine derivatives of light alcohols) generate expected signals from  $5 \times 10^{-1}$  (the effect **E4**) to  $5 \times 10^{-6}$  (the effects **E2** and **E7**) of the <sup>1</sup>H NMR signal obtained after the excitation of the sample by a 90° pulse at the thermodynamic equilibrium. For the effects of relatively large amplitudes, it is sufficient to use, at the beginning of the experiment, the nuclear magnetization at the thermodynamic equilibrium, whereas in the case of the effects of the smallest amplitudes, an application of the hyperpolarization techniques may be required in order to increase the initial nuclear magnetization.

## D.9. References

1. H. Saitô, I. Ando, and A. Ramamoorthy, *Prog. Nucl. Magn. Reson. Spectrosc.*, **57**, 181 (2010)
2. T. J. Wenzel and J. D. Wilcox, *Chirality*, **15**, 256 (2003)
3. K. Bodenhofer, A. Hierlemann, J. Seemann, G. Gauglitz, B. Koppenhoefer, and W. Gopel, *Nature*, **387**, 577 (1997)
4. R. McKendry, M-E. Theoclitou, T. Rayment, C. Abell, *Nature*, **391**, 566 (1998)
5. T. D. James, K. R. A. Samankumara Sandanayake, and S. Shinkai, *Nature*, **374**, 345 (1995)
6. W. H. Pirkle and P. L. Rinaldi, *J. Org. Chem.*, **42**, 3217 (1977)
7. C. Naumann, P. W. Kuchel, *Chem. Eur. J.*, **15**, 12189 (2009)
8. R. Bentley, *Chem. Rev.*, **106**, 4099 (2006)
9. D. A. Varshalovich, A. N. Moskalev, and V. K. Khersonskii, "Quantum Theory of Angular Momentum" (World Scientific, Singapore, 1989)
10. A. D. Buckingham, P. Pyykkö, J. B. Robert, and L. Wiesenfeld, *Mol. Phys.*, **46**, 177 (1982)
11. H. W. Spiess, "Rotation of molecules and nuclear spin relaxation", in Dynamic NMR Spectroscopy (Springer Berlin Heidelberg, Berlin, Heidelberg, 1978), pp. 55–214
12. A. L. Barra, J. B. Robert, and L. Wiesenfeld, *Europhys. Lett.* **5**, 217 (1988)
13. J. B. Robert and A. L. Barra, *Chirality*, **13**, 699 (2001)
14. J. A. Dale, D. L. Dull, and H. S. Mosher, *J. Org. Chem.* **34**(9), 2543 (1969)
15. A. D. Buckingham, *Chem. Phys. Lett.*, **1**, 398 (2004)
16. A. Abragam, "The Principles of Nuclear Magnetism" (Oxford, London, 1961), p. 276
17. M. Goldman, *J. Magn. Reson.*, **149**, 160 (2001)
18. I. Kuprov, N. Wagner-Rundell, and P. J. Hore, *J. Magn. Reson.*, **184**, 196 (2007)
19. S. Blanes, F. Casas, J. A. Oteo, and J. Ros., *Phys. Rep.*, **470**, 151238, (2009)
20. H. Y. Carr and E.M. Purcell, *Phys. Rev.*, **94**, 630 (1954)
21. S. Meiboom and D. Gill, *Rev. Sci. Inst.*, **29**, 688 (1958)
22. N. J. Stone, *At. Data Nucl. Data Tables*, **90**, 75 (2005)
23. K. Jackowski, P. Garbacz, "Nuclear Magnetic Moments and NMR Measurements of Shielding", in: K. Jackowski, M. Jaszurński, (Eds.) Chapter 3, Gas Phase NMR, Royal Society of Chemistry (2016)
24. J. Herzfeld and A. E. Berger, *J. Chem. Phys.*, **73**, 6021 (1980)
25. A. D. Buckingham, *J. Chem. Phys.*, **140**, 011103 (2014)
26. A. D. Buckingham and P. Fischer, *Chem. Phys.*, **324**, 111 (2006)
27. J. D. Walls, R. A. Harris, C. J. Jameson, *Chem. Phys.*, **128**, 154502 (2008)
28. J. D. Walls, R. A. Harris, *J. Chem. Phys.*, **140**, 234201 (2014)

**E. Other scientific achievements**

Scientific publications included in Journal Citation Reports database.

Bibliographic data

|  |   |
|--|---|
| Total number of publications:                    | <b>22</b>                               |
| Total Impact Factor in the year of publication:  | <b>67.989</b>                           |
| Ministry of Science and Higher Education points: | <b>700</b>                              |
| H index:   | <b>7</b>                                |
| Number of citations without self-citations:      | <b>126</b> (23 <sup>rd</sup> July 2018) |
| Number of all citations:                         | <b>158</b> (23 <sup>rd</sup> July 2018) |

Before Ph.D. title (total 6 items)

- P1. **P. Garbacz**, K. Piszczatowski, K. Jackowski, R. Moszyński, M. Jaszuński  
 “Weak intermolecular interactions in gas-phase nuclear magnetic resonance”  
*Journal of Chemical Physics* 135 (2011) 084310  
**MNiSW: 35, IF<sub>2011</sub>: 3.333**

*My contribution to this work is the design and construction of the high pressure system, measurements of the induced shielding by the intermolecular interactions in the gas-phase and analysis of the obtained results. I estimate my contribution to this work as approximately 35 %.*

- P2. P. Fita, **P. Garbacz**, M. Nejbauer, C. Radzewicz, J. Waluk  
 „Ground and excited state double hydrogen transfer in symmetric and asymmetric potentials: comparison of 2,7,12,17-tetra-n-propylporphycene with 9-Acetoxy-2,7,12,17-tetra-n-propyl-porphycene”  
*Chemistry – A European Journal* 17 (2011) 3672  
**MNiSW: 40, IF<sub>2011</sub>: 5.925**

*My contribution to this work is preformation of the measurements of the transient absorption of porphycene derivatives and analysis of the obtained results. I estimate my contribution to this work as approximately 40 %.*

- P3. **P. Garbacz**, K. Jackowski, W. Makulski, R. E. Wasylishen  
 „Nuclear magnetic shielding for hydrogen in selected isolated molecules”  
*Journal of Physical Chemistry A* 116 (2012) 11896  
**MNiSW: 30, IF<sub>2012</sub>: 2.771**

*My contribution to this work preformation of the measurements of shielding of isotopomerologues of hydrogen and disruption of the obtained results in the paper. I estimate my contribution to this work as approximately 30 %.*

- P4. M. Jaszuński, A. Antusek, **P. Garbacz**, K. Jackowski, W. Makulski, M. Wilczek  
„The determination of accurate nuclear magnetic dipole moments and direct measurement of NMR shielding constants”  
*Progress in Nuclear Magnetic Resonance Spectroscopy* 67 (2012) 49  
**MNiSW: 45, IF<sub>2012</sub>: 6.022**  
*My contribution to this work preformation of the measurements of the nuclear magnetic moments and preparation of several figures. I estimate my contribution to this work as approximately 15 %.*
- P5. T. Helgaker, M. Jaszuński, **P. Garbacz**, K. Jackowski  
„The NMR indirect nuclear spin-spin coupling constant of the HD molecule”  
*Molecular Physics* 110 (2012) 2611  
**MNiSW: 20, IF<sub>2012</sub>: 1.670**  
*My contribution to this work preformation of the measurements of the indirect spin-spin coupling constant in the deuterium hydride molecule and analysis of the obtained results. I estimate my contribution to this work as approximately 40 %.*
- P6. M. Jaszuński, M. Repisky, T. B. Demissie, S. Komorovsky, E. Malkin, K. Ruud, **P. Garbacz**, K. Jackowski, W. Makulski  
"Spin-rotation and NMR shielding constants in HCl"  
*Journal of Chemical Physics* 139 (2013) 234302  
**MNiSW: 35, IF<sub>2013</sub>: 3.122**  
*My contribution to this work is preformation of the measurements of the nuclear shielding of <sup>35</sup>Cl i <sup>37</sup>Cl nuclei in the molecule of hydrogen chloride and analysis of the obtained results. I estimate my contribution to this work as approximately 20 %.*

After Ph.D. title (in total 9 articles excluding these related to the habilitation thesis). The star indicates the corresponding author.

- P7. **P. Garbacz**  
“Spin-spin coupling in the HD molecule determined from <sup>1</sup>H and <sup>2</sup>H NMR experiments in the gas-phase”,  
*Chemical Physics* 443 (2014) 1  
**MNiSW: 25, IF<sub>2014</sub>: 1.652**
- P8. **P. Garbacz\***, W. Makulski, M. Jaszuński  
„The NMR spin-spin coupling constant <sup>1</sup>J(<sup>31</sup>P, <sup>1</sup>H) in an isolated PH<sub>3</sub> molecule”  
*Physical Chemistry Chemical Physics* 16 (2014) 21559  
**MNiSW: 35, IF<sub>2014</sub>: 4.493**  
*My contribution to this work is the main idea of the article, measurements of the indirect spin-spin coupling, analysis of the obtained results, preparation of the first version of the paper. I estimate my contribution to this work as approximately 65 %.*

P9. **P. Garbacz**, W. S. Price\*

“<sup>1</sup>H NMR diffusion studies of water self-diffusion in supercooled aqueous sodium chloride solutions”

*Journal of Physical Chemistry A* 118 (2014) 3307

**MNiSW: 30, IF<sub>2014</sub>: 2.693**

*My contribution to this work is preformation of the measurements of the water diffusion coefficient, analysis of the obtained results and preparation of the first version of the manuscript. I estimate my contribution to this work as approximately 60 %.*

P10. **P. Garbacz**, V. V. Terskikh, M. J. Ferguson, G. M. Bernard, M. Kedziorek, R. E. Wasylishen\*

“Experimental characterization of the hydride <sup>1</sup>H shielding tensors for HIrX<sub>2</sub>(PR<sub>3</sub>)<sub>2</sub> and HRhCl<sub>2</sub>(PR<sub>3</sub>)<sub>2</sub>: extremely shielded hydride protons with unusually large magnetic shielding anisotropies”

*Journal of Physical Chemistry A* 118 (2014) 1203

**MNiSW: 30, IF<sub>2014</sub>: 2.693**

*My contribution to this work is the synthesis of the studied iridium and rhodium hydrides, magic angle spinning measurements in the magnetic field B<sub>0</sub>=11.74 T, quantum chemistry computations of the nuclear magnetic shielding hydrides in the Amsterdam Density Functional package. I estimate my contribution to this work as approximately 50 %.*

P11. **P. Garbacz**, K. Jackowski\*,

“NMR shielding of helium-3 in the micropores of zeolites”

*Microporous and Mesoporous Materials* 205 (2015) 52

**MNiSW: 35, IF<sub>2015</sub>: 3.349**

*My contribution to this work is preformation of the measurements of the helium-3 resonance frequency in the microporous materials, analysis of the obtained results, and preparation of the first version of the article. I estimate my contribution to this work as approximately 65 %.*

P12. **P. Garbacz\***, M. Chotkowski, Z. Rogulski, M. Jaszurński

“Indirect Spin–Spin Coupling Constants in the Hydrogen Isotopologues”

*Journal of Physical Chemistry A* 120 (2016) 5549

**MNiSW: 30, IF<sub>2016</sub>: 2.693**

*My contribution to this work is the main idea of the article, measurements of the indirect spin-spin coupling, analysis of the obtained results, preparation of the first version of the paper. I estimate my contribution to this work as approximately 70 %.*

P13. **P. Garbacz\***, W. Makulski

“<sup>183</sup>W nuclear dipole moment determined by gas-phase NMR spectroscopy”

*Chemical Physics* 498–499 (2017) 7

**MNiSW: 25, IF<sub>2017</sub>: 1.767**

*My contribution to this work is the main idea of the article, measurements of the <sup>183</sup>W NMR spectra of tungsten hexafluoride, analysis of the obtained results, and preparation of the first version of the paper. I estimate my contribution to this work as approximately 70 %.*

P14. **P. Garbacz\***, G. Łach

“Isotope Effects on Nuclear Magnetic Shielding in Molecular Hydrogen”

*Journal of Physical Chemistry A* 122 (2018) 590

**MNiSW: 30, IF<sub>2018</sub>: 2.847**

*My contribution to this work is preformation of the isotope effect, analysis of the obtained results, preparation of the first version of the paper. I estimate my contribution to this work as approximately 70 %.*

P15. **P. Garbacz**, M. Misiak, K. Jackowski\*

“Interactions between nitrogen and oxygen molecules studied by gas-phase NMR spectroscopy”

*Chemical Physics Letters* 699 (2018) 194

**MNiSW: 25, IF<sub>2018</sub>: 1.815**

*My contribution to this work is preformation of the <sup>14</sup>N i <sup>15</sup>N NMR spectra (together with dr M. Misiak), analysis of the obtained results, preparation of the first version of the manuscript. I estimate my contribution to this work as approximately 40 %.*



Piotr Garbacz